ORIGINAL ARTICLE

Identification of candidate lung cancer susceptibility genes in mouse using oligonucleotide arrays

W J Lemon*, H Bernert*, H Sun, Y Wang, M You

See end of article for authors' affiliations
*These two authors contributed equally to this work.

Correspondence to: Dr M You, Manuel Tzagournis Medical Research Facility, Room 530, 420W West 12th Avenue, Columbus, Ohio 43210, USA; you-1@medctr.osu.edu

J Med Genet 2002;**39**:644–655

Revised version received 31 May 2002
Accepted for publication 14 June 2002

We applied microarray gene expression profiling to lungs from mouse strains having variable susceptibility to lung tumour development as a means to identify, within known quantitative trait loci (QTLs), candidate genes responsible for susceptibility or resistance to lung cancer. At least eight chromosomal regions of mice have been mapped and verified to be linked with lung tumour susceptibility or resistance. In this study, high density oligonucleotide arrays were used to measure the relative expression levels of >36 000 genes and ESTs in lung tissues of A/J, BALB/cJ, SM/J, C3H/HeJ, and C57BL/6J mice. A number of differentially expressed genes were found in each of the lung cancer susceptibility QTLs. Bioinformatic analysis of the differentially expressed genes located within QTLs produced 28 susceptibility candidates and 22 resistance candidates. These candidates may be extremely helpful in the ultimate identification of the precise genes responsible for lung tumour susceptibility or resistance in mice and, through follow up, humans. Complete data sets are available at http://thinker.med.ohio-state.edu.

Numerous chromosomal regions genetically linked with susceptibility or resistance to pulmonary adenomas have been described in mice using inbred strains showing widely different susceptibilities to formation of both spontaneous and chemical induced lung tumours.[1–3] Susceptibility is intrinsic to the lung itself as shown by the classical experiments involving lung explants from sensitive and resistant mice.[4 5] After carcinogen administration to F_1 mice previously made host to these explants, only the lungs from the sensitive mouse strain developed tumours.[4 5] Matings of sensitive A/J and resistant C57BL/6J mice produce F_1 and F_2 offspring, which are of intermediate sensitivity to tumour induction, thus implicating more than one gene and illustrating that tumour size and number are multigenic quantitative traits.[6] Production of recombinant inbred (RI) lines of A/J (A) and C57BL/6J (B6) mice and subsequent analysis of their tumour sensitivities suggested that three genes, one major and two minor genes, were involved in determining the sensitivity to mouse lung tumour development.[6] Subsequent linkage studies have identified pulmonary adenoma susceptibility (Pas) and pulmonary adenoma resistance (Par) loci. We thus adopt the definition of quantitative trait locus (QTL) as a known chromosomal region in which one or more genes are likely to underlie the linkage.

Listed in table 1 are the selected QTLs that have been mapped in various mouse crosses. A major susceptibility locus was mapped in (A/J × C3H/HeJ) F_2 mice to distal chromosome 6 and was termed the Pas1 locus. This locus produced a maximum logarithm of the likelihood ratio (lod) score of 9 and accounted for approximately 45% of the observed phenotypic variance.[7] A lod score of 3 or greater is considered significant for linkage. Consistent results were obtained in comprehensive linkage studies using (A/J × C57BL/6J) F_2 (60% of variance), (A/J × C57BL/6J) × C57BL/6J (16% of variance), (A/J × *M spretus*) × C57BL/6J (34% of variance), and A × B & B × A RI mice (51% of variance).[8–11] Three other loci were mapped to chromosomes 17, 19, and 9.[8 9] Linkage to a locus on chromosome 17, the site of the putative Pas2 locus, was observed in (A/J × C57BL/6J) F_2, accounting for 8% of the total variance in phenotype. The location of the Pas2 locus is homologous to human chromosome 6p21; potential candidates at this location are the genes for tumour necrosis factor α and β. Similarly, linkages to lung tumour susceptibility were also seen at markers on chromosome 19 (Pas3), accounting for 3% of the phenotypic variation in a study on (A/J × C57BL/6J) × C57BL/6J mice, and 2% of the explained phenotypic variation when (A/J × C57BL/6J) F_2 mice were used. In this latter study, suggestive linkage to a locus on chromosome 9 (Pas4) was determined to explain 4% of the total phenotypic variance.[8 9] Mouse-human synteny for all loci can be examined in detail using the Homology browser at the NCBI (www.ncbi.nlm.nih.gov/Homology).

At present, four Par QTLs have been mapped using F2 or backcross populations of mice, including Parl (chromosome 11), Par2 (chromosome 18), Par3 (chromosome 12), and Par4 (chromosome 4).[12] Par1 is a lung tumour resistance locus that was mapped in (A/J × *M spretus)* × C57BL/6J mice to the retinoic acid receptor-α (*Rara)* gene locus on chromosome 11.[13 14] Contributed by the *M spretus* allele, Par1 gave a maximum lod score of 5.3 accounting for 23% of phenotypic variance when coexpressed with the highly penetrant Pas1 allele of the A/J strain. In mice carrying the *M spretus* instead of the A/J allele of the Pas1 gene, the resistant effect of Par1 on tumour incidence, multiplicity, and volume was lessened by about a half. Par1 behaves like a modulator of Pas1, to some degree subduing the dominant effect of Pas1 on lung tumorigenesis. Par2 was mapped by linkage studies on (A/J × BALB/cByJ) × A/J and (A/JO1aHsd × BALB/cO1aHsd) F_2 mice to chromosome 18 at microsatellite marker D18MIT103. A lod score of 12.2 was reported at this locus, with a phenotypic variance of 38% for resistance to tumour induction.[15] This locus was termed Par2. In our own analysis of (A/JO1aHsd × BALB/cO1aHsd) F_2 mice, Par2 had a significant linkage to lung tumour resistance and produced a maximum lod score of 11.[16] The greatest linkage occurred at the site of the *Dcc* tumour repressor gene.[16] Par3 was mapped to chromosome 12 with a lod score of 6.47, using backcross population between SMXA24 RI mice and A/J mice.[14] Par3 seems to have a stronger resistance to lung tumour induction when coexpressed with the A/J allele of the Par2.[17] Finally, Par4 or Papg1 was mapped

Table 1 Summary of Pas and Par QTLs. Pas QTLs have been largely studied using various genetic crosses of A/J and C57BL/6J; Par 1 and 3 using A/J and SM/J; Par 2 and 4 using A/J and BALB/cJ. Markers flanking the QTLs were taken larger than what some recent fine mapping studies have produced in order to allow identification of multiple genes

				Start marker			End marker				
Locus	Strains	Breeding	Explained variance	Name	Genetic	Celera	Name	Genetic	Celera	Celera Transcripts	Affymetrix Mu74K
Pas 1	A × B6	F2	60%	D6Mit54	48.2	109, 249, 790	D6Mit304	75	142, 276, 365	640	250
Pas 2	A × B6 B6 × A	RI	8	D17Mit23	17	22, 057, 276	D17Mit50	23.2	39, 136, 371	468	119
Pas 3	A × B6	F2	2	D19Mit42	2	6, 828, 495	D19Mit19	25	39, 976, 948	295	61
Pas 4	A × B6	F2	4	D9Mit11	42	82, 499, 293	D9Mit282	72	114, 926, 441	932	213
Par 1	(SMXA × A) × A	BC	~10	D11Mit14	37	69, 772, 571	D11Mit14	59	101, 055, 855	1043	345
Par 2	A × B/c	F2	~50	D18Mit124	32	57, 893, 422	D18Mit4	57	83, 071, 801	373	92
Par 3	(SMXA × A) × A	BC	~10	D12Mit36	13	52, 195, 168	D12Mit6	44	81, 478, 562	457	79
Par 4	A × B/c	F2	~10	D4Mit39	10.6	32, 493, 011	D4Mit77	42.5	83, 848, 148	611	111

to chromosome 4 (D4MIT77) (lod score = 3.0) using (A/JO1aHsd × BALB/cO1aHsd) F_2 mice.[16 18] Linkage on chromosome 4 was strongest at a marker recombinationally inseparable from the *p16*^{INK4a} tumour suppressor gene locus, with the BALB/cJ allele at this locus associated with sensitivity to lung tumour formation.[17]

Identification of candidate Pas and Par genes responsible for the lung cancer susceptibility QTLs proves to be rather difficult. One obstacle is the fact that several hundred genes can be localised to a 20-30 cM QTL region. Fine mapping studies typically assume that one or very few genes are responsible for most of the effect attributed to the QTL. If several genes or a few genes separated by more than a few centimorgans are responsible, fine mapping may prove to be more challenging. Evaluation of differential gene expression and nucleotide polymorphism of such a large number of genes can be a significant challenge. In the present study, we combined the Celera mouse genome sequence and lung cancer genetics with microarray profiling to identify candidate genes. Specifically, we used high density oligonucleotide arrays to detect differential gene expression in lung cancer susceptibility QTL regions for the identification of candidate genes responsible for lung cancer susceptibility or resistance in several relevant mouse strains.

METHODS

Approach

Markers flanking each QTL were located in the Celera (Rockville, MD) mouse genome database (www.celera.com, 6 March and 13 March, 2002 data releases) and transcript information downloaded. Transcripts were matched with Affymetrix probe sets as described below. RNA from selected mouse strains were profiled and the transcripts within each QTL were evaluated for differential expression. Candidacy for differentially expressed transcripts was determined by comparing profiles with published reports as described below.

Animals

Four to six week old mice, one from each of five mouse strains including A/J, SM/J (S), BALB/cJ (Bc), C3H/HeJ, and C57BL/6J (B6) were obtained from The Jackson Laboratory (Bar Harbor, ME). Animals were euthanised one week after arrival. Lungs from these mice were harvested and frozen in liquid nitrogen until RNA analysis.

RNA isolation

Total RNA from lungs of one mouse from each strain was isolated using TRI reagent (Molecular Research Center, Cincinnati, OH). The tissue was frozen in liquid nitrogen, pulverised, then homogenised in 1 ml of TRI reagent, incubated for five minutes at room temperature, followed by addition of 200 µl chloroform, vigorous mixing, and incubation on ice for 15 minutes. The sample was centrifuged at 14 000 rpm for 20 minutes; the aqueous phase was transferred to a fresh tube with an equal volume of isopropanol, and incubated on ice for 30 minutes. After centrifugation at 14 000 rpm for 15 minutes, the RNA pellet was washed in 75% ethanol and dissolved in Rnase free water. The quality of RNA was confirmed on a formaldehyde agarose gel, and the concentration was determined by reading absorbance at 260/280 nm.

Microarray analysis

RNA samples were further purified, labelled, and processed by our microarray core facility according to standard manufacturers' protocols (www.cancergenetics.med.ohio-state.edu/microarray). Singleton cRNA preparations were produced from 30 µg of total RNA from each mouse and 10 µg equivalent aliquots were hybridised to each Affymetrix mouse oligonucleotide array (Santa Clara, CA): Mu74Av2 (A array),

Mu74Bv2 (B array), and Mu74Cv2 (C array). Arrays were then scanned and digitised.

Mapping Affymetrix probe sets to Celera transcript sequences

Transcript IDs, annotations, and transcript sequences for all genes between flanking markers were downloaded from the Celera database. To map Celera transcripts to Affymetrix probe sets, BlastN (www.ncbi.nlm.nih.gov/BLAST/) was used to compare Celera transcript sequences with the Affymetrix "consensus" sequences (www.netaffx.com) for all probe sets of the A, B, and C arrays. An Affymetrix probe set was said to measure a particular Celera transcript under the following conditions: (1) the sum total coverage of blast hits (E<10-4) between an Affymetrix consensus and a Celera transcript included (A) at least 50% of both sequences or (B) 70% of one sequence and, in either case, the longer sequence was no more than 1.5 times as long as the shorter; (2) the probe set met condition 1 for no more than one Celera transcript. This blast method was selected over an annotation matching method since mappings produced with the blast method can be managed by a direct objective scoring scheme, while annotation matching has issues often requiring ad hoc resolution such as annotation differences, redundant accession numbers, etc. For each mapped probe set, the annotation presented here comes from the associated Celera transcript.

Estimates of gene expression

Li-Wong full model estimates (LWF) of gene expression[19 20] were produced for A, B, and C arrays for mRNA samples. To do this, fluorescence intensity data within CEL files were scaled (normalised) by quadratically regressing log intensities for each array against the log of the median spot intensities ($\log(i) = \beta_0 + \beta_1 \log(median) + \beta_2 \log(median)^2$). Median spot intensities were produced for each spot on an array type producing what can be thought of as a pseudo-median array. A arrays were scaled as one group, B arrays another, and C arrays a third group. Estimates of gene expression were produced from the scaled intensity data using a C program available on our web site.

Differential expression and visualisation of gene expression

Expression ratios and a Z scoring method were used to assess differential expression.[21] Ratios of expression between relevant strains for genes within the QTLs were computed. For Pas1-4, A/J and B6 ratios were determined, for Par1 and 3 A/J and S ratios, and for Par2 and 4 A/J and Bc ratios. When more than one probe set met the conditions for association with a particular Celera transcript, the one displaying the greatest fold change between the strains was selected to represent the transcript. This selection provided a means to reduce the false negative rate, which is crucial when identifying candidates.[22] To produce colour images, gene expression values were unit normalised ($(x-\bar{x})/s_x$) across samples of all strains. For Pas 1-4, the A/J and B6 values were retained and displayed via linear colour gradient with cyan indicating values below the mean, red indicating above the mean, and neutral grey near the mean. For Par1 and 3, A/J and S unit normalised values are displayed and for Par2 and 4, A/J and Bc unit normalised values are shown.

Follow up of observed candidates, including validation by RT-PCR or northern blot, is under way, but because of the large number of candidates, it is beyond the scope of this work. Other results from our laboratory and from others indicate good correlation between microarray results and RT-PCR and northern analysis.[23 24]

Estimation of significance

In an approach similar to the "modified t" approach used by Eaves *et al*[22] to analyse the Idd loci for diabetes susceptibility genes, a Z scoring method was used to produce a statistic for comparing two strains within the set of five, and a liberal cut off value was selected to reduce the false negative rate. The Z transformation follows,

$$Z = \frac{g_1 - g_2}{\sqrt{\sigma^2_{g_1} + \sigma^2_{g_2}}}$$

where g_1 and are g_2 the gene expression values for the two strains being compared and σ^2_{g1} and σ^2_{g2} are variances associated with those gene expression values[22] (F Wright, personal communication). Variances were estimated by producing a model of variance from all the gene expression data from all arrays and all samples. A linear model fitting log(variance across strains) to log(mean across strains) from each gene resulted in the model.[20 22] For each expression value, the corresponding variance can be computed and with each pair of expression values, a Z score. The cut off for display was selected as $|Z| > 1$.

Association and concordance with published reports

To identify candidate genes from the several within each QTL passing the Z cut off, annotation was used to search published reports for association of aberrant expression of the gene with cancer. If the observed pattern of expression in the strains was consistent with that of the reported association with cancer, the gene was identified as a candidate. For example, if a gene were a tumour suppressor and array expression showed an increase in the resistant strain, the gene was identified as a candidate for conferring inherent resistance. Note that the nomenclature of Pas or Par does not play a role in this, only the gene's activity does. A tumour suppressor within a Pas locus is a candidate if its expression was higher in the resistant strain. Similarly, an oncogene within a Par locus is a candidate if its expression was higher in the susceptible strain.

RESULTS

Our approach to identifying candidate lung tumour susceptibility and resistance genes builds on previous genetic work, availability of the mouse genome sequence, and genome wide expression profiling. The genome sequence, combined with previously identified QTLs, enabled us to focus our gene expression analysis on transcripts within the regions known to modulate susceptibility and resistance. This reduced the burden of identifying and filtering spurious associations which typically encumber microarray analyses.

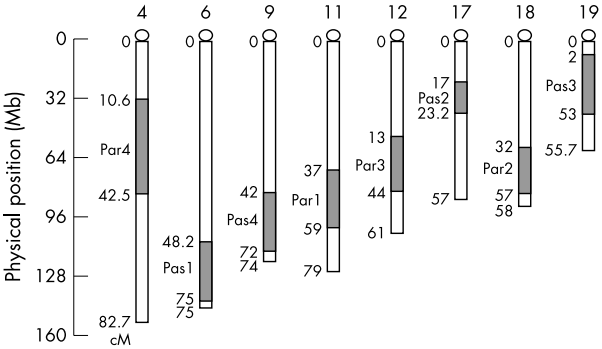

Figure 1 Depiction of the QTLs. Chromosomes are drawn according to physical distance shown on the left with genetic positions adjacent to each figure.

Table 2 Differentially expressed genes within the Pas 1–4 loci. Since the relevant contrast for these loci is between A/J and C57BL/6J, data for these alone are presented.

Affymetrix	Gene expression				Lit		Celera		
Probe set	A/J	C57BL/6J	Fold	Z	A	C	Transcript	Position	Description
Pas1									
160882_at	93.5	59.9	1.6	1.6			mCT16668	111,668,200	Similar to calcium/calmodulin dependent protein kinase I
99534_at	174.9	225.2	0.8	–1.0			mCT20905	112,048,000	Motilin related peptide
163377_at	67.1	49.1	1.4	1.1			mCT17991	119,013,900	CECR2 (hypothetical)
95024_at	156.8	116.8	1.3	1.1	Y		mCT17989	119,506,600	Ubiquitin specific protease 18, 15
99518_at	153.6	228.0	0.7	–1.6			mCT15708	120,721,600	Microfibrillar associated protein 5
94912_at	173.1	120.0	1.4	1.4			mCT51351	121,112,300	Mitochondrial ribosomal protein S21
99635_at	232.0	153.7	1.5	1.7	Y		mCT22535	122,858,900	p33 ING1 homologue
102282_g_at	166.7	122.9	1.4	1.2			mCT22574	123,044,600	CD27L receptor
103499_at	316.6	471.3	0.7	–1.8	Y		mCT6345	123,476,500	von Willebrand factor
102295_at	71.3	45.9	1.6	1.5			mCT6350	124,310,300	Ventricular potassium channel Kv1.5
97504_at	**309.8**	**462.7**	**0.7**	**–1.8**	**Y**	**Y**	**mCT12339**	**124,898,800**	**Cyclin D2**
93095_at	**312.3**	**234.2**	**1.3**	**1.2**	**Y**	**Y**	**mCT12335**	**125,175,000**	**High mobilty group protein 2A, 4**
160456_at	**110.6**	**75.4**	**1.5**	**1.4**	**Y**	**Y**	**mCT50365**	**126,286,900**	**Cyclophilin H**
97761_f_at	110.7	150.8	0.7	–1.2			mCT7594	128,437,000	Natural killer cell receptor LY49GDTM
93893_f_at	57.5	34.4	1.7	1.6	Y		mCT7596	128,527,900	Killer cell lectin-like receptor, subfamily A, member 5
103271_at	63.7	45.2	1.4	1.1	Y		mCT16910	129,272,600	Low density lipoprotein related protein 6
103085_at	175.8	122.7	1.4	1.4			mCT20704	129,952,300	Haem binding protein
96620_at	315.0	247.0	1.3	1.1			mCT21036	130,050,900	Germ cell specific gene 1
160080_r_at	129.0	170.0	0.8	–1.1			mCT8442	131,289,700	RPL44
113727_at	58.2	27.2	2.1	2.3	Y		mCT8441	131,320,300	ATFa associated modulator
93866_s_at	1358.4	2039.5	0.7	–2.3			mCT6144	131,766,500	Matrix Gla protein
100427_at	**143.4**	**104.2**	**1.4**	**1.2**	**Y**	**Y**	**mCT6134**	**132,327,700**	**Protein tyrosine phosphatase BK**
169427_i_at	50.9	33.8	1.5	1.3			mCT6276	135,543,300	Riken cDNA 0610025G13 gene
106298_r_at	16.7	24.1	0.7	–1.0			mCT6279	136,432,400	Organic anion transporter
160741_at	**151.2**	**234.0**	**0.6**	**–1.8**	**Y**	**Y**	**mCT5581**	**137,106,400**	**RecQ protein-like**
100035_at	**299.6**	**520.2**	**0.6**	**–2.5**	**Y**	**Y**	**mCT13800**	**139,928,900**	**ECA39 protein**
97696_r_at	2534.0	2969.4	0.9	–1.0			mCT13794	140,303,300	RPL7 - human
112736_at	**59.6**	**40.6**	**1.5**	**1.3**	**Y**	**Y**	**mCT11838**	**140,747,600**	**Hes related**
93250_r_at	96.4	139.1	0.7	–1.4	Y		mCT11842	141,300,800	Calmodulin 2
111826_at	60.0	82.8	0.7	–1.1			mCT11846	141,390,800	Hypothetical protein FLJ10637
107088_at	280.1	387.1	0.7	–1.4			mCT11853	141,486,800	Riken cDNA 0610007L03 gene
162892_at	51.4	36.2	1.4	1.1			mCT6219	141,840,000	Sterile alpha motif (hypothetical)
Pas2									
165371_i_at	48.6	70.1	0.7	–1.2			mCT18471	23,311,090	Trefoil factor 3, intestinal
115002_at	87.7	65.3	1.3	1.0			mCT18484	23,550,270	Glycerol 3-phosphate permease
97486_at	95.4	137.3	0.7	–1.4	Y		mCT15017	23,861,140	U2AF 35 kDa subunit
114243_at	69.7	46.6	1.5	1.4			mCT15014	24,026,930	Myocardial SNF1-like kinase
110328_at	76.1	53.8	1.4	1.2			mCT14905	24,696,870	Riken cDNA 2310021J05
102689_at	**468.9**	**369.2**	**1.3**	**1.1**	**Y**	**Y**	**mCT22852**	**26,406,370**	**Tapasin**
95158_at	**530.0**	**729.0**	**0.7**	**–1.6**	**Y**	**Y**	**mCT22857**	**26,425,580**	**KE2**
102992_at	**123.6**	**167.0**	**0.7**	**–1.2**	**Y**	**Y**	**mCT22855**	**26,485,130**	**H2-K region expressed gene 6**
103616_at	211.7	156.2	1.4	1.2			mCT22850	26,497,970	Procollagen, type XI, alpha 2
103035_at	110.7	152.8	0.7	–1.2			mCT22863	26,634,000	TAP1-g7
104429_at	101.5	141.5	0.7	–1.3			mCT4541	26,743,420	Histocompatibility 2, O region beta locus
92652_at	**103.8**	**71.2**	**1.5**	**1.4**	**Y**	**Y**	**mCT4529**	**27,211,740**	**Notch4**
99652_at	251.7	333.3	0.8	–1.2			mCT14181	27,714,700	NG26
101416_f_at	252.8	337.3	0.7	–1.3			mCT14134	27,747,330	BAT4
93840_at	241.2	169.4	1.4	1.5			mCT14185	27,754,750	Apolipoprotein M
115138_at	**95.2**	**67.5**	**1.4**	**1.2**	**Y**	**Y**	**mCT17665**	**28,013,740**	**MHC psoriasis candidate protein**
96212_at	142.5	95.7	1.5	1.5			mCT17672	28,374,830	CG16787 gene product
95124_i_at	**130.2**	**189.9**	**0.7**	**–1.5**	**Y**	**Y**	**mCT17677**	**28,417,670**	**Regulator of cullins 1**
101341_at	**593.1**	**786.9**	**0.8**	**–1.4**	**Y**	**Y**	**mCT23544**	**28,933,180**	**Histocompatibility 2, M region locus 9**
103987_at	63.4	45.2	1.4	1.1			mCT23038	29,279,660	Myelin/oligodendrocyte glycoprotein precursor
93041_at	95.9	71.8	1.3	1.0			mCT23261	30,162,000	Mini chromosome maintenance deficient 4 homologue
94111_r_at	57.9	123.7	0.5	–2.6			mCT23260	30,325,400	Similar to ZNF14 (KOX 6)
93348_at	107.8	76.3	1.4	1.3	Y		mCT49663	31,898,120	Phosphoglycerate kinase 2
94730_at	27.5	12.1	2.3	2.2			mCT20042	31,983,740	Acidic epididymal glycoprotein 1
114707_at	8.6	13.8	0.6	–1.2			mCT12126	32,320,720	Riken cDNA 2610528M18Rik
116771_at	**90.3**	**66.8**	**1.4**	**1.1**	**Y**	**Y**	**mCT11932**	**35,423,590**	**Ectonucleotide pyrophosphatase/ phosphodiesterase 4**
108262_at	71.8	95.8	0.7	–1.0			mCT11931	35,506,800	Chloride intracellular channel 5
94041_at	**172.7**	**125.7**	**1.4**	**1.3**	**Y**	**Y**	**mCT5959**	**36,985,830**	**Heterogeneous nuclear ribonucleoprotein K**
114726_at	**108.3**	**167.2**	**0.6**	**–1.7**	**Y**	**Y**	**mCT13097**	**39,168,870**	**CDC5-like**
95359_at	793.5	982.0	0.8	–1.1			mCT12707	39,344,620	Heat shock protein 84
Pas3									
161384_r_at	888.5	684.5	1.3	1.3			mCT15177	40,463,040	Hermansky-Pudlak syndrome protein
111898_at	51.8	35.7	1.5	1.2			mCT16304	41,789,800	Hypothetical protein FLJ10998
94065_at	98.7	70.0	1.4	1.2			mCT9896	42,071,970	Acyl-CoA desaturase 1
97389_at	**78.6**	**106.6**	**0.7**	**–1.1**	**Y**	**Y**	**mCT1056**	**42,740,910**	**cdc25 homologue A (*S cerevisiae*)**
115138_at	**95.2**	**67.5**	**1.4**	**1.2**	**Y**	**Y**	**mCT14682**	**43,709,310**	**Semaphorin 4G**

Cont.

Table 2 continued

Affymetrix	Gene expression				Lit		Celera		
Probe set	A/J	C57BL/6J	Fold	Z	A	C	Transcript	Position	Description
102796_at	116.0	158.5	0.7	–1.2			mCT10907	44,440,830	Nucleoplasmin 3
107249_at	**29.1**	**20.5**	**1.4**	**1.0**	**Y**	**Y**	**mCT10892**	**44,950,270**	**Golgi specific brefeldin A resistance factor 1**
94334_f_at	442.1	353.8	1.2	1.0			mCT22402	45,702,150	66 kDa neurofilament protein NF-66
113579_at	75.2	99.8	0.8	–1.0			mCT22401	46,183,310	Hypothetical protein FLJ22559
97819_at	238.1	496.5	0.5	–3.1			mCT5611	46,546,310	Glutathione-S-transferase-like
108925_at	55.5	35.9	1.5	1.4			mCT19627	47,290,880	VPS10 domain receptor
99162_at	83.6	120.0	0.7	–1.3			mCT22431	52,008,630	Splicing factor 30,survival of motor neuron related
103029_at	190.6	69.2	2.8	3.4	Y		mCT22341	52,537,490	Apoptosis protein MA-3 (PDCD4)
102635_at	17.2	229.6	0.1	–5.6			mCT19862	54,116,940	Vesicle transport through interaction with t-SNAREs 1 homologue
102151_at	**163.0**	**240.4**	**0.7**	**–1.6**	**Y**	**Y**	**mCT19826**	**55,318,310**	**Adrenergic receptor, beta 1**
110339_at	62.5	46.1	1.4	1.0			mCT19828	55,630,530	Actin binding LIM protein 1, isoform a
Pas4									
169427_i_at	50.9	33.8	1.5	1.3			mCT12262	83,884,330	T box transcription factor TBX18
105097_at	228.3	149.0	1.5	1.7			mCT19945	95,049,700	Claudin 18
160932_at	**40.8**	**15.1**	**2.7**	**2.7**	**Y**	**Y**	**mCT19764**	**95,904,200**	**Tyrosine kinase adaptor protein 1**
92489_at	**141.7**	**105.5**	**1.3**	**1.1**	**Y**	**Y**	**mCT19766**	**96,358,630**	**Stromal antigen 1**
100101_at	198.8	267.1	0.7	–1.3			mCT19754	96,852,280	Small nuclear ribonucleoprotein polypeptide A
103085_at	**175.8**	**122.7**	**1.4**	**1.4**	**Y**	**Y**	**mCT15895**	**98,688,030**	**Similar to topoIIBP**
160326_at	125.6	178.6	0.7	–1.4			mCT15894	98,732,280	CDV-3B
116123_at	269.5	341.6	0.8	–1.1			mCT3740	100,503,100	Riken cDNA 2310041H06 gene
163306_at	58.4	39.7	1.5	1.3			mCT3725	100,736,700	Hypothetical protein XP_039534
160352_at	270.1	189.8	1.4	1.5			mCT20224	101,833,700	Poly(rC)-binding protein 4
99534_at	**174.9**	**225.2**	**0.8**	**–1.0**	**Y**	**Y**	**mCT15938**	**102,938,800**	**G(i) alpha 2**
110292_at	93.4	69.1	1.4	1.1			mCT16206	102,975,600	NAT-1
112736_at	59.6	40.6	1.5	1.3			mCT16182	103,385,700	Hypothetical protein FLJ12565
94167_at	196.6	250.7	0.8	–1.0	Y		mCT18729	103,642,900	eNOS
100444_at	**79.9**	**105.5**	**0.8**	**–1.0**	**Y**	**Y**	**mCT18731**	**103,697,300**	**Cyclin dependent kinase 5**
108911_at	**78.3**	**116.1**	**0.7**	**–1.4**	**Y**	**Y**	**mCT18933**	**103,862,400**	**SMARC D3**
111826_at	**60.0**	**82.8**	**0.7**	**–1.1**	**Y**	**Y**	**mCT18907**	**104,395,600**	**Wiskott-Aldrich syndrome homologue binding protein**
105375_at	8.3	13.7	0.6	–1.3			mCT18909	104,513,100	6-phosphofructo-2-kinase/ fructose-2,6-biphosphatase 4
101115_at	86.8	128.1	0.7	–1.4			mCT20670	105,153,300	Lactoferrin precursor
98482_at	**77.8**	**44.6**	**1.7**	**1.8**	**Y**	**Y**	**mCT20658**	**105,440,600**	**Parathyroid hormone receptor**
98254_f_at	856.3	1138.9	0.8	–1.5			mCT52401	106,253,100	Similar to Ribosomal protein L7a (*H sapiens*)
103647_at	148.3	209.1	0.7	–1.4			mCT6130	108,921,500	Acid beta-galactosidase
115311_at	42.4	26.2	1.6	1.5			mCT6129	109,441,300	Related to glycerophosphate dehydrogenase.
93880_at	110.9	75.4	1.5	1.4			mCT21847	112,331,400	Tbr2
98302_at	213.4	272.5	0.8	–1.0			mCT19669	113,463,800	Sodium channel, type X, alpha polypeptide

Probe set, Li-Wong full model estimates of gene expression, fold change, and Z score are indicated in columns 1–5. Columns 6 and 7 indicate if the gene has an association with cancer in published reports and, if so, if its observed differential expression is concordant with that of its association. The final columns are the Celera annotation for the transcript. A/J is the susceptible strain in all cases. Candidates (bold) are those having expression concordant with that published

The eight previously mapped QTLs are summarised in table 1 and shown pictorially in fig 1 using physical position of flanking markers in the Celera mouse genome. Susceptibility loci (Pas1-4) are located respectively on chromosomes 6, 17, 19, and 9. Resistance loci (Par1-4) are located respectively on chromosomes 11, 18, 12, and 4. The columns contain first the loci, followed by the strains involved in original mapping, breeding method used during mapping, approximate phenotypic variance explained by alleles of the crossed strains, proximal flanking markers, their genetic positions in MGD (www.jax.org), and physical positions in the Celera database. Next appear the distal flanking markers and their positions. The final two columns contain the number of transcripts found in the Celera genome between the markers and the number of those transcripts found to be uniquely represented on the microarrays.

In total, 4819 transcripts were found within the eight QTLs in the Celera Discovery database and 1270 of these were found to be represented on one or more arrays. LWF estimates of gene expression were determined and fold change between relevant strains computed to assess differential expression.

Table 2 illustrates gene expression differences for transcripts within the Pas 1-4 QTLs in order of physical position. Pas QTLs depict comparison of expression between A/J and B6 (fig 2). Table 3 depicts expression of transcripts within the Par 1-4 QTLs also ordered by position. Par1 and 3 depict comparison between A/J and S and Par1 and 2 depict comparison between A/J and Bc (fig 3). Both tables 2 and 3 provide details of Li-Wong full model estimates of gene expression, statistics, and annotation derived from Celera.

DISCUSSION

Pas1-4

Pas1

In Pas1-4, A/J is the susceptible strain and B6 the resistant one. Tumour suppressor candidates will have shown higher expression in B6, while oncogene candidates will have shown higher expression in A/J. *Pas1* is a major susceptibility locus based on the genetic linkage studies in several crosses. Because of its location, the *K-ras* gene became a candidate for the *Pas1*. However, *K-ras* had a Z score of 0.6 and thus did not make the list of candidates on the basis of expression. Many models implicating *K-ras* postulate a central role of mutation in tumorigenesis which may not be manifest in normal gene expression under the conditions here. A/J and B6 carry different alleles of *K-ras*, but differential expression was not detected in this experiment. Genes that did show differential

Table 3 Similar to table 2, except for the relevant contrasts. Par 1 and 3 involve A/J and SM/J while Par 2 and 4 involve A/J and BALB/cJ. In all cases except Par 4, A/J is the susceptible strain

Affymetrix	Gene expression				Lit		Celera		
Probe set	A/J	SM/J	Fold	Z	A	C	Transcript	Position	Description
Par1									
100729_at	1709.0	1208.8	1.4	2.0			mCT11594	70,066,180	RPL26
102216_at	**154.1**	**101.8**	**1.5**	**1.6**	**Y**	**Y**	**mCT11607**	**70,329,560**	**12-lipoxygenase**
110656_at	488.4	370.0	1.3	1.3			mCT22709	70,909,700	Sentrin/SUMO specific protease
95555_at	104.0	136.2	0.8	–1.0			mCT11964	79,393,870	UNC-119 homologue (*C elegans*)
94761_at	110.6	49.6	2.2	2.6			mCT52567	83,127,990	Monocytic cytokine FIC
94166_g_at	159.8	262.8	0.6	–2.0			mCT7613	83,256,700	Small inducible cytokine A1
94146_at	750.9	995.9	0.8	–1.5			mCT16927	84,654,840	Small inducible cytokine A4
109329_at	12.9	19.8	0.6	–1.2			mCT11724	85,989,200	Ubiquitin specific protease
132134_at	25.9	18.3	1.4	1.0			mCT63872	90,225,430	GIOT-1
94110_f_at	251.0	152.2	1.6	2.0			mCT23795	90,389,780	Zinc finger protein s11-6
98761_i_at	**130.8**	**89.5**	**1.5**	**1.4**	**Y**	**Y**	**mCT23795**	**90,389,780**	**Zinc finger protein s11-6**
100713_at	61.4	34.1	1.8	1.9			mCT54937	90,478,550	BC37295_1
160096_at	**153.9**	**248.3**	**0.6**	**–1.9**	**Y**	**Y**	**mCT7476**	**97,537,590**	**Speckle type POZ protein**
94240_i_at	**753.1**	**572.9**	**1.3**	**1.4**	**Y**	**Y**	**mCT12415**	**99,422,870**	**RPL29/HIP**
111892_r_at	66.2	46.0	1.4	1.2			mCT12712	99,520,370	KIAA0775
94025_at	440.2	315.8	1.4	1.5			mCT12735	100,079,800	Macropain subunit beta 3
98998_r_at	835.2	1038.9	0.8	–1.2			mCT22409	102,446,600	Hair keratin acidic 5
163459_at	21.7	14.3	1.5	1.2			mCT22420	102,785,700	Riken cDNA 4921517C11
99444_at	402.6	592.9	0.7	–1.8			mCT19970	103,576,900	Receptor-activity modifying protein 2
93803_at	383.7	538.5	0.7	–1.6			mCT19897	103,646,900	Macropain 28 subunit, 3
93066_at	**166.2**	**120.3**	**1.4**	**1.3**	**Y**	**Y**	**mCT22039**	**104,768,700**	**Granulin**
109821_f_at	218.6	167.0	1.3	1.1			mCT6549	105,187,500	Proteasome beta type subunit 5
Par2									
99500_at	336.5	134.1	2.5	3.5			mCT21401	58,328,380	Sodium/potassium/chloride transporters
160081_at	733.2	348.7	2.1	3.4			mCT19134	60,175,410	RPL44
96764_at	**192.8**	**138.4**	**1.4**	**1.3**	**Y**	**Y**	**mCT19135**	**60,772,940**	**Interferon-g induced GTPase**
165190_f_at	292.6	184.0	1.6	1.9			mCT4726	61,138,540	RPS14
103477_at	113.7	76.8	1.5	1.4			mCT4721	61,382,610	Caudal type homeo box 1
104354_at	185.9	255.6	0.7	–1.3	Y		mCT4715	61,468,440	c-fms
95935_at	159.9	10.8	14.8	5.3			mCT4705	61,558,260	Diastrophic dysplasia
99650_at	385.9	209.0	1.8	2.6			mCT13340	61,915,330	Hypothetical protein XP_046994
93193_at	**232.5**	**91.4**	**2.5**	**3.3**	**Y**	**Y**	**mCT49747**	**62,531,770**	**Beta-2 adrenergic receptor**
103893_at	**289.6**	**179.3**	**1.6**	**2.0**	**Y**	**Y**	**mCT21247**	**62,842,980**	**5-HT (serotonin) receptor**
98113_at	474.7	312.5	1.5	1.9			mCT49712	64,190,020	Macropain subunit beta 1
95070_at	93.8	66.5	1.4	1.2			mCT19071	64,762,360	Asparaginyl-tRNA synthetase
163131_at	29.9	16.7	1.8	1.6			mCT10477	67,480,240	Riken cDNA 2810405I11
92429_at	**94.7**	**70.0**	**1.4**	**1.1**	**Y**	**Y**	**mCT5163**	**68,680,940**	**Melanocortin 2 receptor**
160833_at	**166.0**	**79.1**	**2.1**	**2.7**	**Y**	**Y**	**mCT8975**	**70,950,710**	**Methyl-CpG binding domain protein 2**
100621_at	236.0	153.0	1.5	1.8			mCT49617	74,634,430	RPL10A
94778_at	300.8	119.3	2.5	3.5			mCT55393	74,794,640	RPS11
93095_at	**312.3**	**199.9**	**1.6**	**1.9**	**Y**	**Y**	**mCT9020**	**75,562,950**	**High mobility group protein 1**
169427_i_at	50.9	18.5	2.8	2.8			mCT50963	76,674,120	Riken cDNA 0610025G13
95705_s_at	137.7	269.6	0.5	–2.6			mCT49635	78,828,430	Similar to CG6244 gene product
140417_at	546.1	984.0	0.6	–2.9	Y		mCT21388	78,849,820	Partitioning defective protein 6, alpha
98168_at	1159.1	829.0	1.4	1.8	Y		mCT21125	79,637,650	RPL7a; surfeit 3
98852_at	542.6	418.6	1.3	1.2	Y		mCT21123	79,744,900	Spalt
100732_at	984.8	793.8	1.2	1.1			mCT49634	79,773,310	RPS8
96311_at	252.9	151.6	1.7	2.1			mCT2560	81,221,470	Myelin basic protein
99872_s_at	1973.3	1243.7	1.6	2.6			mCT51216	82,350,360	Ferritin light chain1
Par3									
97181_f_at	660.7	1143.2	0.6	–2.8			mCT6323	55,700,680	Antigen LEC-A - mouse
168094_i_at	152.9	108.6	1.4	1.3			mCT17763	62,133,540	HSPC327
170035_at	96.4	72.0	1.3	1.1			mCT10566	66,254,020	Similar to C1-tetrahydrofolate synthase
92909_at	**282.0**	**198.1**	**1.4**	**1.5**	**Y**	**Y**	**mCT4371**	**75,045,630**	**Placental growth factor**
Par4									
101651_at	149.0	111.2	1.3	1.1			mCT9802	39,054,870	Ciliary neurotrophic factor receptor
104615_at	48.5	70.5	0.7	–1.3			mCT9810	39,153,330	Similar to galactose-1-phosphate uridyl transferase
104616_g_at	173.0	376.2	0.5	–3.1			mCT9810	39,153,330	Similar to galactose-1-phosphate uridyl transferase
100710_at	373.5	223.6	1.7	2.2	Y		mCT18829	39,448,380	Valosin containing protein
109821_f_at	218.6	109.6	2.0	2.6			mCT18833	39,496,760	Stomatin-like protein 2
101886_f_at	1366.1	980.2	1.4	1.8			mCT18854	39,885,870	CD72 antigen
102033_at	174.3	131.0	1.3	1.1			mCT18841	39,887,490	Testis specific protein kinase 1
100605_at	221.4	150.4	1.5	1.6			mCT18837	39,959,110	Skeletal muscle beta-tropomyosin
97002_f_at	93.8	64.6	1.5	1.3			mCT18834	40,217,400	Olfactory receptor 37a
97001_r_at	64.9	45.5	1.4	1.2			mCT18840	40,270,280	Olfactory receptor 37c
100579_s_at	216.5	153.8	1.4	1.4			mCT17967	40,451,270	Clathrin light chain A1
97924_at	193.9	150.5	1.3	1.0			mCT18007	40,475,760	UDP-N-acetylglucosamine-2-epimerase/ N-acetylmannosamine kinase

Cont.

Table 3 continued

Affymetrix	Gene expression				Lit		Celera		
Probe set	A/J	SM/J	Fold	Z	A	C	Transcript	Position	Description
92628_at	617.2	370.1	1.7	2.4			mCT49891	41,844,870	RPL36
92349_at	**79.7**	**55.9**	**1.4**	**1.2**	**Y**	**Y**	**mCT12508**	**42,312,200**	**IGFBP-like protein**
92384_at	86.0	45.6	1.9	2.1			mCT13922	42,671,340	Xeroderma pigmentosum, complementation group A
94401_s_at	15.4	25.5	0.6	–1.4			mCT2768	42,916,920	Haemogen
93548_at	136.1	82.8	1.6	1.8			mCT6236	43,965,870	Riken cDNA 1190006C12
104273_at	162.3	351.0	0.5	–3.1			mCT12849	46,213,260	Similar to amino acid n-acyltransferase
98570_at	52.6	34.7	1.5	1.3			mCT4703	49,433,900	Nascent polypeptide associated complex alpha polypeptide
97198_at	99.7	192.1	0.5	–2.5			mCT1837	49,649,520	abc-1
99162_at	83.6	62.3	1.3	1.0			mCT51070	50,801,170	Hypothetical protein XP_017858
94240_i_at	753.1	533.0	1.4	1.7			mCT18653	51,795,030	RPL29
165619_r_at	6.6	15.4	0.4	–2.0			mCT6237	53,232,650	Actin-like 7a
96143_at	40.1	22.3	1.8	1.7	Y		mCT2186	53,551,990	Erythrocyte protein band 4.1-like 4b
92807_at	1044.9	680.3	1.5	2.2	Y		mCT2181	54,431,540	Thioredoxin
166368_at	65.7	47.7	1.4	1.1			mCT2179	54,471,070	Riken cDNA 4930429J24
94763_at	112.3	69.8	1.6	1.7			mCT16138	54,774,370	Muscle localised kinase 2
101910_f_at	129.9	204.2	0.6	–1.8			mCT18276	56,436,830	Major urinary protein 4
94110_f_at	251.0	160.2	1.6	1.8			mCT13881	56,835,390	ZFP-37
92974_at	94.1	70.1	1.3	1.1			mCT13881	56,835,390	ZFP-37
101877_at	129.7	55.9	2.3	2.8			mCT13880	57,003,100	Copper transporter 1
100408_at	**81.8**	**50.7**	**1.6**	**1.6**	**Y**	**Y**	**mCT6036**	**57,284,400**	**DNA polymerase epsilon subunit 3**
94045_at	**115.0**	**69.4**	**1.7**	**1.8**	**Y**	**Y**	**mCT6028**	**57,887,030**	**Bikunin**
100437_g_at	243.5	169.2	1.4	1.5	Y		mCT6038	58,087,310	Orosomucoid 1
101136_at	160.2	216.7	0.7	–1.2	Y		mCT18762	58,561,280	Tumour necrosis factor superfamily, member 8
101759_at	**51.5**	**69.7**	**0.7**	**–1.0**	**Y**	**Y**	**mCT12635**	**62,899,270**	**TCP-1-alpha**
98901_at	154.4	119.4	1.3	1.0			mCT49201	64,236,180	CGI-35
97909_at	**298.7**	**410.2**	**0.7**	**–1.4**	**Y**	**Y**	**mCT6339**	**64,446,380**	**Stathmin**
107446_at	**505.3**	**260.8**	**1.9**	**2.9**	**Y**	**Y**	**mCT6342**	**64,917,520**	**EGF-like domain multiple 5**
98333_at	1383.6	1087.2	1.3	1.3			mCT18717	65,828,720	RPS18
102425_at	82.4	36.6	2.3	2.6			mCT1623	66,695,350	Hypothetical protein XP_005490
93847_at	**116.7**	**75.5**	**1.5**	**1.6**	**Y**	**Y**	**mCT6233**	**69,792,470**	**Protein-tyrosine-phosphatase receptor delta**
97956_g_at	**346.2**	**217.1**	**1.6**	**2.0**	**Y**	**Y**	**mCT8849**	**74,689,350**	**Tyrosinase related**
100728_at	185.4	442.5	0.4	–3.5			mCT8927	75,123,540	Multiple PDZ domain
97939_at	251.3	141.7	1.8	2.3			mCT8914	77,109,010	Riken cDNA 2610202L11
97751_f_at	258.2	380.4	0.7	–1.7			mCT3200	77,879,180	Glyceraldehyde-3-phosphate dehydrogenase
98589_at	477.8	261.9	1.8	2.6	Y		mCT1071	81,176,840	Adipose differentiation related
163145_at	51.5	26.6	1.9	2.0			mCT6119	82,300,740	AF9
110716_at	22.8	32.4	0.7	–1.1			mCT6118	83,135,710	Hypothetical protein DJ1198H6.2
102149_f_at	**151.2**	**103.2**	**1.5**	**1.5**	**Y**	**Y**	**mCT6126**	**83,202,950**	**Interferon alpha family, gene B**
101791_f_at	278.9	211.0	1.3	1.2			mCT6126	83,202,950	Interferon alpha family, gene B
110656_at	488.4	279.7	1.7	2.5			mCT6122	83,230,580	KIAA1354
93557_at	86.7	53.8	1.6	1.6			mCT12990	83,481,020	Selenophosphate synthetase 2
98789_at	**106.9**	**75.5**	**1.4**	**1.3**	**Y**	**Y**	**mCT124933**	**84,760,902**	**Cyclin dependent kinase inhibitor p16INK4a**

expression by the stated criteria are: hes related protein, cyclophilin H, protein tyrosine phosphatase BK, matrix Gla protein, recQ, and ECA39. Hes related protein is a basic helix-loop-helix protein with a Notch binding site that is responsive to Notch activation.[25 26] Notch4, a candidate in Pas2 below, has been shown to be a site of insertion for viral intercisternal A particles. Insertion can result in a constitutively active Notch4 which can ultimately drive transformation to a highly invasive phenotype.[27] Cyclophilin H is a paralogue of Pin1, which has been shown to interfere directly with the association of beta-catenin and Apc resulting in (1) increases of beta-catenin, cyclin D1, c-Myc, and (2) a decrease in apoptosis as a consequence of ubiquitination of IkappaB.[28] Pin1 has been shown to be up regulated in breast tumours. Protein tyrosine phosphatase BK is of the receptor type and does not react with serine residues.[29] Its function is otherwise unknown, but the central role of phosphorylation in cell signalling indicates that it remains a candidate. Matrix gla is a cell adhesion molecule that has been shown to be down regulated in colorectal cancer, although its role in tumorigenesis is not known.[30] RecQ is a DNA damage repair enzyme in which missense alleles in humans have been shown to alter the risk of lung cancer by two-fold.[31] ECA39/Bcat1, branched chain amino acid aminotransferase, catabolyses branched chain amino acids and produces ketoacids which at high levels induce apoptosis.[32] ECA39 is a c-myc target and has been implicated in c-myc regulated apoptosis.[32]

Pas2

Pas2 QTL is located at the H-2 locus whose haplotypes correlate with the incidence and multiplicity of mouse lung tumour induction.[8] The expected candidates are TNFα and β. Neither made the Z cutoff (TNFα Z=0.43, TNFβ Z=0.65). Among the oncogenic candidates passing the Z cutoff are Notch4, heterogeneous nuclear ribonucleoprotein K (protein K), and ENPP4. Candidate tumour suppressors are regulator of cullins 1 and cdc5-like. The several differentially expressed MHC genes are MHC psoriasis candidate protein, histocompatibility 2 M region locus 9, H2-K region expressed gene 6, histocompatibility 2 O region beta locus, and tapasin. Candidacy of these genes was determined as follows. Protein K can be bound by the Par2 candidate high mobility group protein 1, which can also bind p53 and another Par2 candidate methyl-CpG binding domain protein 2.[33] Protein K has pluripotent function that links translation, cell cycle, and apoptosis. Protein K dependent repression of translation can be modulated through phosphorylation by ERK.[34] Protein K is a target of JNK which has a role in apoptosis[35] and protein K transcription can be induced by EGF.[36] ENPP4 (Autotaxin), a myc target which induces metastasis in the co-presence of

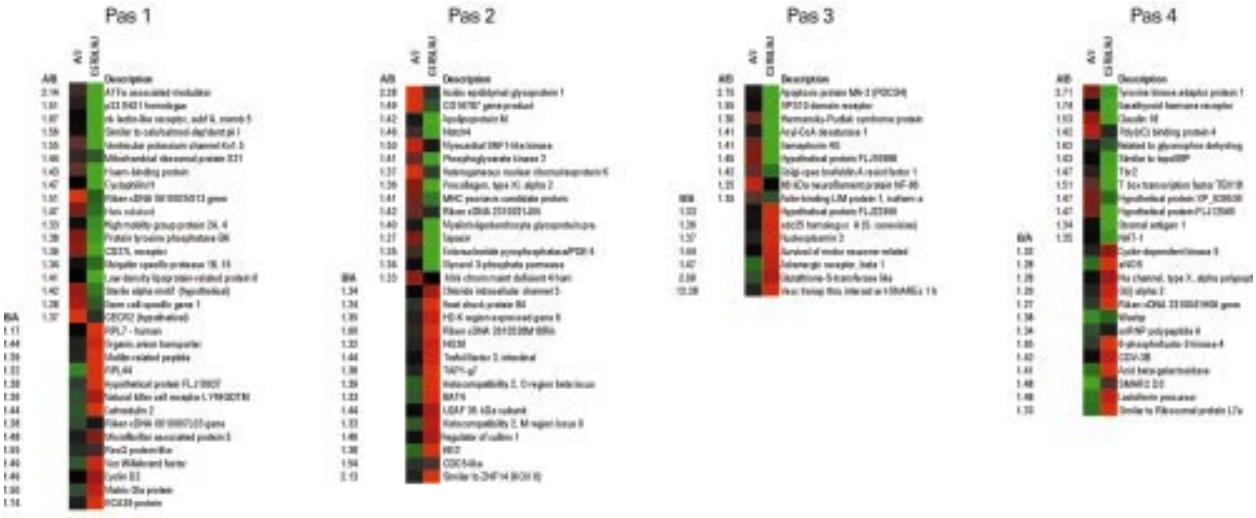

Figure 2 Coloured image of gene expression for transcripts in the Pas 1-4 QTLs from A/J and C57BL/6J. The leftmost column in each panel denotes the fold change from A/J to C57BL/6J, while the adjacent column denotes the fold change from C57BL/6J to A/J. Colour denotes the number of standard deviations that expression differs from the mean expression for all five strains. Green denotes below average expression, red denotes above average expression, and black denotes near average expression. An edited version of the annotation provided by Celera for each transcript appears to the right of each image.

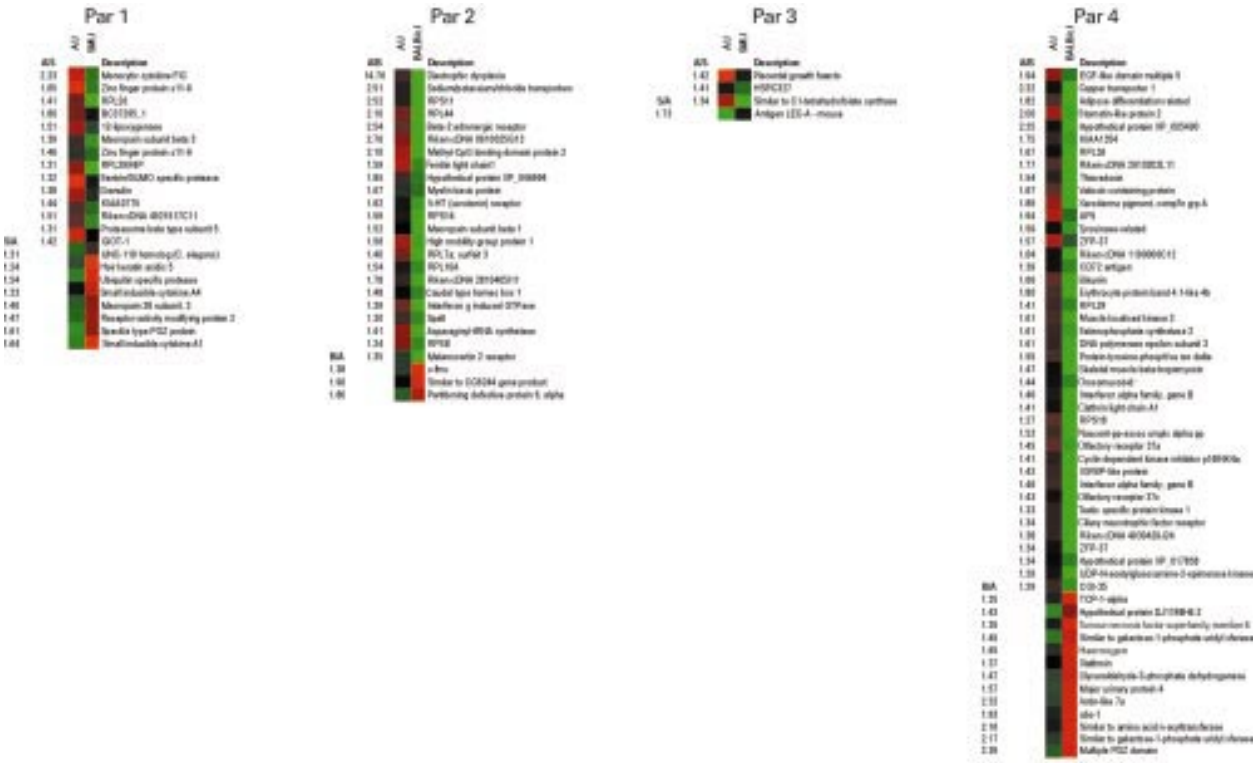

Figure 3 Coloured image of gene expression for transcripts in the Par1 and 3 QTLs from A/J and SM/J in Par2 and 4 from A/J and BALB/cJ. Values and colours are the same as those described for figure 2.

retinoic acid, is also a candidate.[37] Regulator of cullins 1 is a member of the von Hippel-Lindau tumour suppressor complex which regulates, in part, ubiquitination of IκB and consequent activation of NFκB.[38] The function of cdc5-like is not known, but by homology has a likely role in regulating the cell cycle which indicates that it should remain a candidate. MHC genes can play roles in transformation and metastasis in many ways, so those genes are all left as candidates.

Pas3

Pas3 was first described by Devereux *et al*[9] as flanked by D19MIT42 and D19MIT19 using linkage analysis of N-ethyl-N- nitrosourea treated (A/J × C57BL/6J) Fl × C57BL/6J backcross progeny. This observation was later confirmed by Festing *et al*[16] using urethane treated (A/J × C57BL/6J) F2 mice. Pas3 oncogenic candidates include golgi specific brefeldin A resistance factor 1 and semaphorin 4G. Discordantly expressed non-candidate genes having interesting

backgrounds include apoptosis protein MA-3 and cdc25 homologue A. Brefeldin A is a drug used to induce apoptosis in adenocarcinomas through a process that blocks ADP-ribosylation of proteins in the golgi apparatus. When this process is blocked, proteins awaiting ribosylation accumulate, eventually triggering an "ER stress" induced apoptosis signal involving caspases 9 and 12. The BFA resistance factor transfers ribosylation factors to proteins such that the drug effect is mitigated.[39] The precise role of semaphorin 4G is not known, but other semaphorins, such as M-semaH, are implicated in metastatic potential.[40] The beta 1 adrenergic receptor, along with the beta 2 receptor in Par2, is a candidate although publications on the role of these in apoptosis is mixed. Some results suggest that beta 2 receptor expression is the key to sensitising cells to cisplatin induced apoptosis,[41] others that coactivation of beta 1 and beta 2 receptors correlates with NK resistance to metastasis,[42] and others that they both work along with cyclooxygenase 2 to produce arachidonic acid metabolites that induce apoptosis.[43] Incidentally, COX-2 (chromosome 1) showed very low or no expression in any of the tissues.

Interestingly, this locus enhances lung tumour multiplicity more significantly when K-ras has a heterozygous genotype as compared with resistant homozygotes. The oncogenic candidates primarily affect apoptosis pathways. With heterozygous Ras and susceptible Pas3, one would have a situation in which cells have the propensity to divide and be resistant to apoptosis. This could be a model for the relationship between Pas3 and Pas1.

Pas4

Pas4 was mapped by Festing *et al*.[16] The expected candidate associated with this locus in gene mapping studies is TGFβ receptor II, but was not differentially regulated in this study. Oncogene candidates are SH2/SH3 adapter protein (*Nck*), parathyroid hormone receptor, similar to topoisomerase II binding protein, and *NAT-1*. *Nck*, a known proto-oncogene, seems to play pluripotent roles in processes including translation and actin polymerisation.[44–46] Nck has been shown to bind Wasbp, a Pas4 tumour suppressor candidate listed below, which also performs a role in actin polymerisation.[45] Parathyroid hormone and parathyroid hormone receptor have both been shown in vitro to be expressed in type II alveolar epithelial cells and in an adenocarcinoma cell line and thus have been postulated as forming an autocrine loop.[47] TopBP1 has been shown to be involved in DNA damage repair and checkpoint control.[48] This function may reduce rates of apoptosis.[48] Interestingly, another topoisomerase II binding protein found in Par4, DNA polymerase epsilon subunit 3, has a human homologue, YB-1, whose expression pattern parallels that of PCNA in adenocarcinoma.[49] This provides two topoIIBPs which promote cell survival or proliferation. NAT1, a highly polymorphic N-acetyltransferase known to activate and detoxify tobacco carcinogens, has been indicated for genotyping to assess risk for adenocarcinoma.[50]

Pas4 tumour suppressor candidates are G protein alpha I 2, cdk5, SMARC D3, and Wiskott-Aldrich syndrome binding protein. Gαi2 does not have a clear role in cancer, although some work has been done on oncogenic cell signalling through pathways involving it. Should it have a role, these data suggest a tumour suppressive one. Cdk5 has been suggested to have a role in apoptosis of glioblastoma multiforme cells, as well as in non-neural cells through a cAMP dependent pathway.[51] Wasbp was discussed above. SMARC D3, involved in chromatin remodelling, has been postulated to operate as a tumour suppressor in mice and humans.[52]

A number of Pas4 genes appear to be associated with cancer through cytoskeletal interactions. For example, Nck-1 connects the ras pathway with cytoskeletal signals.[53] Wiskott-Aldrich syndrome involves dysregulation of cytoskeletal signalling through actin binding and WASBP is a candidate.[54] Stromal antigens, also related to cytoskeletin, can be signalling molecules during metastasis. SMARCs are actin dependent chromatin regulators of which SMARC D3 is differentially regulated in the direction favouring carcinogenesis. It has been suggested from data in *Drosphila* that topoisomerase II and actin can regulate chromatin remodelling and thus gene transcription.[55] The theme for Pas4 appears to be a linkage between cytoskeletal signals and chromatin or gene expression. Although TGF β receptor was not seen differentially regulated here, it has been suggested that one effect of TGF during tumorigenesis is to induce cytoskeletal reorganisation.[56]

Par1-4

Par1

Par1 was first mapped by Manenti *et al*[13] by crossing Pas1 positive A/J × *M Spretus* F1 mice with B6 mice. Later, Patear *et al*[14] published results using backcrosses of ((A/J × S RI) × A/J)F1 × A/J which confirmed Par1 on chromosome 11 and mapped Par3 on chromosome 12. In Par1, A/J is the susceptible strain and SM/J the resistant strain. Par1 contains the retinoic acid receptor and its allele has been suggested to modulate the Pas1 allele.[12] RARα showed no difference in expression between A/J and SM/J. Oncogene candidates are 12-lipoxygenase, zinc finger protein s11-6, granulin, and ribosomal protein L29. Inhibition of 12-lipoxygenase has been shown to produce apoptosis in prostate cancer, gastric cancer, and other cancers.[57 58] It has been shown that a 12-lipoxygenase metabolite, 12-HETE, phosphorylates ERK which consequently induces proliferation of cancer cells and this is postulated as a mechanism for tumour cell proliferation in vivo.[58] In Pas1, several ERK pathway modulators are present including cyclophilin H, cyclin D2, and ECA39, any or all of which could link these loci in the fashion suggested by previous genetic studies. The candidate zinc finger s11-6 seems to have unknown function. However, with a nearly certain role in DNA binding, it remains a candidate. Granulin has a precursor form called PC cell derived growth factor (PCDGF) which has been shown to mediate oestradiol induced mitosis in breast cancer by activating MAPK and cyclin D1.[59] Here there is a plausible link to Pas1 via cyclin D2, rather than cyclin D1. Expression of RPL29, a heparin sulphate interacting protein, has been correlated in colorectal carcinoma with metastatic status.[60]

The Par1 candidate tumour suppressor is speckle type POZ protein. SPOP has been suggested through bioinformatics to interact with the tumour necrosis alpha receptor and thus may play a role in apoptosis.[61]

Par2

In Par2, A/J is the susceptible strain and BALB/cJ the resistant. The candidate oncogenes are beta-2 adrenergic receptor, methyl-CpG binding domain protein 2, serotonin receptor, high mobility group protein 1, and interferon G induced GTPase. All except the serotonin receptor were discussed above. Serotonin receptor has been implicated as having opposing dual roles in cancer. On the one hand, 5HT stimulation produces vasoconstriction and thus limits blood supply to tumours. On the other hand, tumour cells expressing receptor produce an autocrine loop that supports aggressive proliferation.[62] These data, assuming it is the Par2 gene, suggest that its role in proliferation is more important. Expression of IFN gamma induced GTPase has been shown to correlate with proliferation rate of fibroblast cells in vitro.[63] This is consistent with an oncogenic role.

The major gene on distal chromosome 18 has previously been reported,[15 64] though chromosome 18 markers are only occasionally deleted in mouse lung tumours.[64 65] Expected candidate genes are *Dcc* (deleted in colorectal cancer) and

homologues of *DPC4* and *JVI8-1* which have been shown to be deleted in a small number of non-small cell lung cancers.[64] The *Mcc* (mutated in colon cancer) and *Apc* (adenomatous polyposis coli) genes, shown to have decreased expression in mouse lung tumours,[66] map to a different region of chromosome 18. In this study, only *Dcc* passed the Z cutoff but was not considered a candidate as its expression is higher in A/J. In this study, we observed differential expression of high mobility group protein 1 which non-specifically binds DNA and also binds p53, and by computer analysis performed by others putatively binds methyl-CpG binding domain protein 2, and heterogeneous nuclear ribonucleoprotein K.[33] Since some of these are activators and others repressors, this suggests that the transcriptional machinery may have a different set point in A/J versus Bc or B6.

Par3

In Par3, one candidate oncogene appears, placental growth factor. P1GF has been shown to bind to VEGF1 receptor and to play an important role promoting angiogenesis in wound healing, cancer, etc.[67] Genetic studies have shown that having the Par2 A/J allele and the Par3 SM/J allele confers increased resistance to tumorigenesis.[12] The data here are as consistent as follows. The SM/J allele of P1GF, having lower expression, would be expected to result in a lower rate of angiogenesis, thus inhibiting tumour growth. Simultaneously, the A/J allele of Par2, providing increased expression of serotonin receptor, would augment vasoconstriction, further inhibiting tumour growth in spite of other factors supporting tumour proliferation.

Par4

In Par4, BALB/cJ is the susceptible strain, A/J the resistant, since, in a backcross, hybrid mice containing the A/J allele for Par4 are more resistant to tumours than those carrying the BALB/cJ allele.[16] Increased resistance produced by the A/J allele is pronounced in males. Interestingly, this locus is closely linked to D4Mit77 and therefore also to the Cdkn2a (pI6INK4a) locus.[68] Chromosome 4 markers in this region are often deleted in mouse lung adenocarcinomas,[17 65 69] skin carcinomas,[70] and hepatocellular carcinomas,[71] and the human homologue on chromosome 9p21 is similarly deleted in some human tumours.[72] Our results are consistent with this in that p16INK4a shows higher expression in A/J. Candidate tumour suppressors are EGF-like domain multiple 5, bikunin, DNA polymerase epsilon subunit 3 (pole3), tyrosinase related protein 1, interferon alpha gene B, and IGFBP-like protein. Once again, candidacy was determined as follows. EGF-like domain multiple 5 is an uncharacterised gene, but it may play a role in growth factor signalling, so it remains a candidate. Bikunin has been shown to inhibit metastasic processes when overexpressed.[73] However, in colorectal carcinoma, expression was observed in both tumour and normal tissue with no discernible difference.[74] Pole3 was discussed above. Tyrosinase related protein 1 is involved in melanogenesis and coat colour. Interferon alpha induces apoptosis and some data suggest that it is mediated by a c-myc dependent pathway.[75] Insulin-like growth factor binding proteins are known to inhibit cell growth and promote apoptosis by binding the growth factors and thus blocking them from interacting with their receptors.[76] This role is consistent with the results here.

Candidate oncogenes are T complex protein 1 alpha and stathmin. TCP-1, a chaperonin involved in cytoskeletal protein folding, has been shown to be upregulated in colon cancer and to be a member of the complex that includes von Hippel-Lindau (VHL) protein.[77 78] Stathmin overexpression has been reported to correlate with proliferation in ovarian cancer.[79] Overall, the candidates observed in this data set are involved in cell cycling or apoptosis and seem to be clustered near the position of D4Mit77.

General

The most efficient and effective way to look for differences in expression of the genes in a given QTL is through microarray technology. It can be speculated that at least some causative genes will be differentially expressed, so candidates obviously can be sought among genes found to be differentially expressed. This dataset illustrates that candidates come from several regulatory areas including apoptosis, cytoskeletal organisation, chromatin modelling, and cell cycle. As such, susceptibility and resistance to cancer involves a constellation of factors, some interacting, and failure of any one can lead to carcinogenesis. This observation may impact on both treatment and further research. It may be that the next stage in personalised medicine for cancer will initially involve a tumour work up to establish whether the primary aberration involves the cell cycle, apoptosis, or cytoskeleton and from there, which gene and finally how best to intervene. In other words, start with functional assays then follow up with genotyping and intervention strategies. The concentration, diversity, and multiplicity of genes found within these QTLs to be reported in other studies as aberrant in cancerous samples suggests that fine genetic mapping may be a problematical approach. Fine mapping may be most appropriate for conditions with a strong suggestion of monogenicity.

Our statistical threshold was selected to reduce the false negative rate, since omission of a candidate is more problematical than carrying forward non-candidates. Just as methods to reduce the false positive rate, such as Bonferroni correction, increase the false negative rate, our choice of reducing the false negative rate necessarily increases the false positive rate. Managing false positives was accomplished in several ways. First we focused analysis on genetically determined QTLs. Second, we leveraged published reports to apply what has already been observed about specific genes in cancer. This approach has the potential pitfall that our analysis may be restricted by current thinking. However, we have noted all the genes which have been observed to be associated with cancer, even when expression here appears discordant with reported observations. Some of these, such as ATFa modulator in Pas1 and PDCD4 in Pas3, would be interesting to follow up on.

The apparent concentration of highly cancer associated genes within these QTLs, regardless of their concordant or discordant expression in this study, suggests a model for carcinogenesis in which genomic position plays a major role. Suppose the genomic positions of these QTLs were used during mitosis for both DNA replication and another DNA involving process, such as transcription or segregation, in a fashion that permitted local replication errors at a rate much higher than that for more distant positions. This would produce a situation in which mutations are regionally concentrated at these foci and thus could affect any number of proximate genes. Any such regions containing genes involved in sensitive, necessary pathways would be associated with cancer, but analysis of any given tumour would often show several mutated genes. Carcinogenesis per se would still involve failure of cell cycle regulation or apoptosis, but the mechanism for mutation would involve an interference of one DNA involved process such as transcription or segregation with DNA replication. These candidate genes are currently being verified using RT-PCR or northern analysis and the results will be reported in the near future.

SUMMARY

In summary, we have identified a number of candidates for lung cancer susceptibility based on their concordant allele specific differential gene expression. In addition, this study shows the usefulness of genome wide expression profiling using microarrays in conjunction with QTL mapping in the identification of genes responsible for genetic traits. We believe that some of the identified candidates are functionally

relevant and that their expression concords with genetic studies and thus should be selected for further examination. Accordingly, a series of experiments based on the information from the present study are under way to determine allelic variations and allele specific functional differences in lung tumorigenesis.

ACKNOWLEDGEMENTS

We are grateful to F Wright, A de la Chapelle, and G Stoner for their critical reading of this manuscript and helpful discussions. This work was supported by NIH grants R01CA58554 (MY), R01CA78797 (YW), and P30CA16058.

Authors' affiliations

W J Lemon, H Bernert, H Sun, M You, Division of Human Cancer Genetics, The Ohio State University Comprehensive Cancer Center, 420 West 12th Avenue, Columbus, Ohio 43210, USA
Y Wang, School of Public Health, The Ohio State University Comprehensive Cancer Center, 420 West 12th Avenue, Columbus, Ohio 43210, USA

REFERENCES

1 **Andervont HB**. Pulmonary tumors in mice. V. Further studies on the influence of heredity upon spontaneous and induced lung tumors. *Public Health Rep* 1938;**53**:232.
2 **Malkinson AM**. The genetic basis of susceptibility to lung tumors in mice. *Toxicology* 1989;**54**:241-71.
3 **Shimkin MB**. Pulmonary tumors in experimental animals. *Adv Cancer Res* 1955;**3**:223.
4 **Heston WE**, Dunn TB. Tumor development in susceptible strain A and resistant strain L lung transplants. *J Natl Cancer Inst* 1951;**11**:1057.
5 **Shapiro JR**, Kirschbaum AJ. Intrinsic tissue response to induction of pulmonary tumors. *Cancer Res* 1951;**11**:644.
6 **Malkinson AM**, Nesbitt MN, Skamene E. Susceptibility to urethane-induced pulmonary adenomas between A/J and C57BL/6J mice: use of AxB and BxA recombinant inbred lines indicating a three-locus genetic model. *J Natl Cancer Inst* 1985;**75**:971-4.
7 **Gariboldi M**, Manenti G, Canzian F, Falvella FS, Radice MT, Pierotti MA, Della PG, Binelli G, Dragani A. A major susceptibility locus to murine carcinogenesis maps on chromosome 6. *Nat Genet* 1993;**3**:132-6.
8 **Festing MFW**, Yang A, Malkinson AM. At least four genes and sex are associated with susceptibility to urethane-induced adenomas in mice. *Genet Res* 1994;**64**:99-106.
9 **Devereux TR**, Wiseman RW, Kaplan N, Garren S, Foley JF, White CM, Anna C, Watson MA, Patel A, Jarchow S, Maronpot RR, Anderson MW. Assignment of a locus for mouse lung tumor susceptibility to proximal chromosome 19. *Mamm Genome* 1994;**5**:749-55.
10 **Manenti G**, Falvella FS, Gariboldi M, Dragani TA, Pierotti MA. Different susceptibility to lung tumorigenesis in mice with an identical K-ras 2 intron 2. *Genomics* 1995;**29**:438-44.
11 **Lin L**, Festing MFW, Devereux TR, Crist K, Christiansen S, Wang Y, Yang A, Svenson K, Paigen B, Malkinson A, You M. Additional evidence that the K-ras protooncogene is a candidate for the major mouse pulmonary adenoma susceptibility (Pas1) gene. *Exp Lung Res* 1998;**24**:481-97.
12 **Herzog CR**, Lubet RA, You M. Genetic epigenetic alterations in mouse lung tumors: implications for cancer chemoprevention. *J Cell Biochem* 1997;**28**:49-63.
13 **Manenti G**, Gariboldi M, Elango R, Fiorino A, De Gregorio L, Falvella FS, Hunter K, Housman D, Pierotti MA, Dragani TA, Genetic mapping of a pulmonary adenoma resistance (Par1) in mouse. *Nat Genet* 1996;**12**:455-7.
14 **Pataer A**, Nishimura M, Kamoto T, Ichioka K, Sato M, Hiai H. Genetic resistance to urethan-induced pulmonary adenomas in SMXA recombinant inbred mouse strains. *Cancer Res* 1997;**57**:2904-8.
15 **Obata M**, Nishimori H, Ogawa K, Lee GH. Identification of the Par2 (pulmonary resistance locus) on mouse chromosome 18, a major genetic determinant for lung carcinogen resistance in BALB/cByJ mice. *Oncogene* 1996;**13**:1599-604.
16 **Festing MFW**, Lin L, Devereux TR, Gao F, Yang A, Anna CH, White CM, Malkinson AM, You M. At least four loci associated with susceptibility to the chemical induction of lung adenomas in mice. *Genomics* 1998;**53**:129-36.
17 **Herzog CR**, You M. Sequence variation and chromosomal mapping of the murine p16INK4a tumor suppressor gene. *Mamm Genome* 1997;**8**:65-6.
18 **Manenti G**, Gariboldi M, Fiorino A, Zanesi N, Pierotti MA, Dragani TA. Genetic mapping of lung cancer modifier loci specifically affecting tumor initiation and progression. *Cancer Res* 1997;**57**:4164-6.
19 **Li C**, Wong WH, Model-based analysis of oligonucleotide arrays: expression index computation and outlier detection. *Proc Natl Acad Sci USA* 2001;**98**:31-6.
20 **Lemon WJ**, Palatini JJT, Krahe R, Wright FA, Theoretical and experimental comparisons of gene expression indexes for oligonucleotide microarrays. *Bioinformatics* (in press).
21 **Notterman DA**, Alon U, Sierk AJ, Levine AJ, Transcriptional gene expression profiles of colorectal adenoma, adenocarcinoma, and normal tissue examined by oligonucleotide arrays. *Cancer Res* 2001;**61**:3124-30.
22 **Eaves IA**, Wicker LS, Ghandour G, Lyons PA, Peterson LB, Todd JA, Glynne RJ. Combining mouse congenic strains and microarray gene expression analyses to study a complex trait: the NOD model of type 1 diabetes. *Genome Res* 2002;**12**:232-43.
23 **Huang Y**, Prasad M, Lemon WJ, Hampel H, Wright FA, Kornacker K, LiVolsi V, Frankel W, Kloos RT, Eng C, Pellegata NS, de la Chapelle A. Gene expression in papillary thyroid carcinoma reveals highly consistent profiles. *Proc Natl Acad Sci USA* 2001;**98**:15044-9.
24 **Mutch DM**, Berger A, Mansourian R, Rytz A, Roberts MA, Microarray data analysis: a practical approach for selecting differentially expressed genes. *Genome Biol* 2001;**2**:preprint 0009.1–0009.31.
25 **Iso T**, Sartorelli V, Poizat C, Iezzi S, Wu HY, Chung G, Kedes L, Hamamori Y. HERP, a novel heterodimer partner of HES/E(spl) in Notch signaling. *Mol Cell Biol* 2001;**21**:6080-9.
26 **Iso T**, Sartorelli V, Chung G, Shichinohe T, Kedes L, Hamamori Y. HERP, a new primary target of Notch regulated by ligand binding. *Mol Cell Biol* 2001;**21**:6071-9.
27 **Callahan R**, Raafat A. Notch signaling in mammary gland tumorigenesis. *J Mammary Gland Biol Neoplasia* 2001;**6**:23-36.
28 **Ryo A**, Nakamura M, Wulf G, Liou YC, Lu KP. Pin1 regulates turnover and subcellular localization of beta-catenin by inhibiting its interaction with APC. *Nat Cell Biol* 2001;**3**:793-801.
29 **Tomemori T**, Seki N, Suzuki Y, Shimizu T, Nagata H, Konno A, Shirasawa T. Isolation and characterization of murine orthologue of PTP-BK. *Biochem Biophys Res Commun* 2000;**276**:974-81.
30 **Fan C**, Sheu D, Fan H, Hsu K, Allen Chang C, Chan E. Down-regulation of matrix Gla protein messenger RNA in human colorectal adenocarcinomas. *Cancer Lett* 2001;**165**:63-9.
31 **Butkiewicz D**, Rusin M, Enewold L, Shields PG, Chorazy M, Harris CC. Genetic polymorphisms in DNA repair genes and risk of lung cancer. *Carcinogenesis* 2001;**22**:593-7.
32 **Eden A**, Benvenisty N. Involvement of branched-chain amino acid aminotransferase (Bcat1/Eca39) in apoptosis. *FEBS Lett* 1999;**457**:255-61.
33 **Dintilhac A**, Bernues J. HMGB1 interacts with many apparently unrelated proteins by recognizing short amino acid sequences. *J Biol Chem* 2002;**277**:7021-8.
34 **Habelhah H**, Shah K, Huang L, Ostareck-Lederer A, Burlingame AL, Shokat KM, Hentze MW, Ronai Z. ERK phosphorylation drives cytoplasmic accumulation of hnRNP-K and inhibition of mRNA translation. *Nat Cell Biol* 2001;**3**:325-30.
35 **Habelhah H**, Shah K, Huang L, Burlingame AL, Shokat KM, Ronai Z. Identification of new JNK substrate using ATP pocket mutant JNK and a corresponding ATP analogue. *J Biol Chem* 2001;**276**:18090-5.
36 **Mandal M**, Vadlamudi R, Nguyen D, Wang RA, Costa L, Bagheri-Yarmand R, Mendelsohn J, Kumar R. Growth factors regulate heterogeneous nuclear ribonucleoprotein K expression and function. *J Biol Chem* 2001;**276**:9699-704.
37 **Dufner-Beattie J**, Lemons RS, Thorburn A. Retinoic acid-induced expression of autotaxin in N-myc-amplified neuroblastoma cells. *Mol Carcinog* 2001;**30**:181-9.
38 **Spiegelman VS**, Stavropoulos P, Latres E, Pagano M, Ronai Z, Slaga TJ, Fuchs SY. Induction of beta-transducin repeat-containing protein by JNK signaling and its role in the activation of NF-kappaB. *J Biol Chem* 2001;**276**:27152-8.
39 **Claude A**, Zhao BP, Kuziemsky CE, Dahan S, Berger SJ, Yan JP, Arnold AD, Sullivan EM, Melancon P. GBF1: a novel Golgi-associated BFA-resistant guanine nucleotide exchange factor that displays specificity for ADP-ribosylation factor 5. *J Cell Biol* 1999;**146**:71-84.
40 **Christensen CR**, Klingelhofer J, Tarabykina S, Hulgaard EF, Kramerov D, Lukanidin E. Transcription of a novel mouse semaphorin gene, M-semaH, correlates with the metastatic ability of mouse tumor cell lines. *Cancer Res* 1998;**58**:1238-44.
41 **Bando T**, Fujimura M, Kasahara K, Ueno T, Matsuda T. Selective beta2-adrenoceptor agonist enhances sensitivity to cisplatin in non-small cell lung cancer cell line. *Oncol Rep* 2000;**7**:49-52.
42 **Ben-Eliyahu S**, Shakhar G, Page GG, Stefanski V, Shakhar K. Suppression of NK cell activity and of resistance to metastasis by stress: a role for adrenal catecholamines and beta-adrenoceptors. *Neuroimmunomodulation* 2000;**8**:154-64.
43 **Schuller HM**, Plummer HK III, Bochsler PN, Dudric P, Bell JL, Harris RE, Co-expression of beta-adrenergic receptors and cyclooxygenase-2 in pulmonary adenocarcinoma. *Int J Oncol* 2001;**19**:445-9.
44 **Kebache S**, Zuo D, Chevet E, Larose L, Modulation of protein translation by Nck-1. *Proc Natl Acad Sci USA* 2002;**99**:5406-11.
45 **Rohatgi R**, Nollau P, Ho HY, Kirschner MW, Mayer BJ. Nck and phosphatidylinositol 4,5-bisphosphate synergistically activate actin polymerization through the N-WASP-Arp2/3 pathway. *J Biol Chem* 2001;**276**:26448-52.
46 **Rockow S**, Tang J, Xiong W, Li W. Nck inhibits NGF and basic FGF induced PC12 cell differentiation via mitogen-activated protein kinase-independent pathway. *Oncogene* 1996;**12**:2351-9.
47 **Hastings RH**, Summers-Torres D, Cheung TC, Ditmer LS, Petrin EM, Burton DW, Spragg RG, Li J, Deftos LJ. Parathyroid hormone-related protein, an autocrine regulatory factor in alveolar epithelial cells. *Am J Physiol* 1996;**270**:L353-61.

48 **Yamane K**, Wu X, Chen J. A DNA damage-regulated BRCT-containing protein, TopBP1, is required for cell survival. *Mol Cell Biol* 2002;**22**:555-66.
49 **Gu C**, Oyama T, Osaki T, Kohno K, Yasumoto K. Expression of Y box-binding protein-1 correlates with DNA topoisomerase IIalpha and proliferating cell nuclear antigen expression in lung cancer. *Anticancer Res* 2001;**21**:2357-62.
50 **Wikman H**, Thiel S, Jager B, Schmezer P, Spiegelhalder B, Edler L, Dienemann H, Kayser K, Schulz V, Drings P, Bartsch H, Risch A. Relevance of N-acetyltransferase 1 and 2 (NAT1, NAT2) genetic polymorphisms in non-small cell lung cancer susceptibility. *Pharmacogenetics* 2001;**11**:157-68.
51 **Sandal T**, Stapnes C, Kleivdal H, Hedin L, Doskeland SO. A novel, extra neuronal role for cyclin-dependent protein kinase 5 (cdk5): modulation of cAMP-induced apoptosis in rat leukemic cells. *J Biol Chem* 2002;**21**:21.
52 **Klochendler-Yeivin A**, Muchardt C, Yaniv M. SWI/SNF chromatin remodeling and cancer. *Curr Opin Genet Dev* 2002;**12**:73-9.
53 **Li W**, Fan J, Woodley DT, Nck/Dock: an adapter between cell surface receptors and the actin cytoskeleton. *Oncogene* 2001;**20**:6403-17.
54 **Stewart DM**, Tian L, Nelson DL. Linking cellular activation to cytoskeletal reorganization: Wiskott-Aldrich syndrome as a model. *Curr Opin Allergy Clin Immunol* 2001;**1**:525-33.
55 **Kroeger PE**, Rowe TC. Analysis of topoisomerase I and II cleavage sites on the Drosophila actin and Hsp70 heat shock genes. *Biochemistry* 1992;**31**:2492-501.
56 **Moustakas A**, Stournaras C. Regulation of actin organisation by TGF-beta in H-ras-transformed fibroblasts. *J Cell Sci* 1999;**112**:1169-79.
57 **Pidgeon GP**, Kandouz M, Meram A, Honn KV. Mechanisms controlling cell cycle arrest and induction of apoptosis after 12-lipoxygenase inhibition in prostate cancer cells. *Cancer Res* 2002;**62**:2721-7.
58 **Wong BC**, Wang WP, Cho CH, Fan XM, Lin MC, Kung HF, Lam SK, 12-Lipoxygenase inhibition induced apoptosis in human gastric cancer cells. *Carcinogenesis* 2001;**22**:1349-54.
59 **Lu R**, Serrero G. Mediation of estrogen mitogenic effect in human breast cancer MCF-7 cells by PC-cell-derived growth factor (PCDGF/granulin precursor). *Proc Natl Acad Sci USA* 2001;**98**:142-7.
60 **Wang Y**, Cheong D, Chan S, Hooi SC. Heparin/heparan sulfate interacting protein gene expression is up-regulated in human colorectal carcinoma and correlated with differentiation status and metastasis. *Cancer Res* 1999;**59**:2989-94.
61 **Zapata JM**, Pawlowski K, Haas E, Ware CF, Godzik A, Reed JC. A diverse family of proteins containing tumor necrosis factor receptor-associated factor domains. *J Biol Chem* 2001;**276**:24242-52.
62 **Vicaut E**, Laemmel E, Stucker O. Impact of serotonin on tumour growth. *Ann Med* 2000;**32**:187-94.
63 **Gorbacheva VY**, Lindner D, Sen GC, Vestal DJ. The interferon (IFN)-induced GTPase, mGBP-2. Role in IFN-gamma-induced murine fibroblast proliferation. *J Biol Chem* 2002;**277**:6080-7.
64 **Devereux TR**, Anna CH, Patel AC, White CM, Festing MF, You M, Smad4 (homolog of human DPC4) and Smad2 (homolog of human JV18-1): candidates for murine lung tumor resistance and suppressor genes. *Carcinogenesis* 1997;**18**:1751-5.
65 **Hegi ME**, Devereux TR, Dietrich WF, Cochran CJ, Lander ES, Foley JF, Maronpot RR, Anderson MW, Wiseman RW. Allelotype analysis of mouse lung carcinomas reveals frequent allelic losses on chromosome 4 and an association between allelic imbalances on chromosome 6 and K-ras activation. *Cancer Res* 1994;**54**:6257-64.
66 **Oreffo VI**, Robinson S, You M, Wu MC, Malkinson AM. Decreased expression of the adenomatous polyposis coli (Apc) and mutated in colorectal cancer (Mcc) genes in mouse lung neoplasia. *Mol Carcinog* 1998;**21**:37-49.
67 **Carmeliet P**, Moons L, Luttun A, Vincenti V, Compernolle V, De Mol M, Wu Y, Bono F, Devy L, Beck H, Scholz D, Acker T, DiPalma T, Dewerchin M, Noel A, Stalmans I, Barra A, Blacher S, Vandendriessche T, Ponten A, Eriksson U, Plate KH, Foidart JM, Schaper W, Charnock-Jones DS, Hicklin DJ, Herbert JM, Collen D, Persico MG. Synergism between vascular endothelial growth factor and placental growth factor contributes to angiogenesis and plasma extravasation in pathological conditions. *Nat Med* 2001;**7**:575-83.
68 **Quelle DE**, Ashmun RA, Hannon GJ, Rehberger PA, Trono D, Richter KH, Walker C, Beach D, Sherr CJ, Serrano M. Cloning and characterization of murine p16INK4a and p15INK4b genes. *Oncogene* 1995;**11**:635-45.
69 **Herzog CR**, Soloff EV, McDoniels AL, Tyson FL, Malkinson AM, Haugen-Strano A, Wiseman RW, Anderson MW, You M. Homozygous codeletion and differential decreased expression of p15INK4b, p16INK4a-alpha and p16INK4a-beta in mouse lung tumor cells. *Oncogene* 1996;**13**:1885-91.
70 **Linardopoulos S**, Street AJ, Quelle DE, Parry D, Peters G, Sherr CJ, Balmain A. Deletion and altered regulation of p16INK4a and p15INK4b in undifferentiated mouse skin tumors. *Cancer Res* 1995;**55**:5168-72.
71 **Kitagawa T**, Miyasaka K, Kanda H, Yasui H, Hino O. Hepatocarcinogenesis in rodents and humans. *J Cancer Res Clin Oncol* 1995;**121**:511-15.
72 **Woloschak M**, Yu A, Xiao J, Post KD. Frequent loss of the P16INK4a gene product in human pituitary tumors. *Cancer Res* 1996;**56**:2493-6.
73 **Kobayashi H**. Suppression of urokinase expression and tumor metastasis by bikunin overexpression. *Hum Cell* 2001;**14**:233-6.
74 **Kataoka H**, Itoh H, Uchino H, Hamasuna R, Kitamura N, Nabeshima K, Koono M. Conserved expression of hepatocyte growth factor activator inhibitor type-2/placental bikunin in human colorectal carcinomas. *Cancer Lett* 2000;**148**:127-34.
75 **Yasuoka Y**, Naomoto Y, Yamatsuji T, Takaoka M, Kimura M, Uetsuka H, Matsubara N, Fujiwara T, Gunduz M, Tanaka N, Haisa M. Combination of tumor necrosis factor alpha and interferon alpha induces apoptotic cell death through a c-myc-dependent pathway in p53 mutant H226br non-small-cell lung cancer cell line. *Exp Cell Res* 2001;**271**:214-22.
76 **Grimberg A**, Cohen P, Role of insulin-like growth factors and their binding proteins in growth control and carcinogenesis. *J Cell Physiol* 2000;**183**:1-9.
77 **Yokota S**, Yamamoto Y, Shimizu K, Momoi H, Kamikawa T, Yamaoka Y, Yanagi H, Yura T, Kubota H. Increased expression of cytosolic chaperonin CCT in human hepatocellular and colonic carcinoma. *Cell Stress Chaperones* 2001;**6**:345-50.
78 **Hansen WJ**, Ohh M, Moslehi J, Kondo K, Kaelin WG, Welch WJ. Diverse effects of mutations in exon II of the von Hippel-Lindau (VHL) tumor suppressor gene on the interaction of pVHL with the cytosolic chaperonin and pVHL-dependent ubiquitin ligase activity. *Mol Cell Biol* 2002;**22**:1947-60.
79 **Price DK**, Ball JR, Bahrani-Mostafavi Z, Vachris JC, Kaufman JS, Naumann RW, Higgins RV, Hall JB, The phosphoprotein Op18/stathmin is differentially expressed in ovarian cancer. *Cancer Invest* 2000;**18**:722-30.